International Journal of Computational and Experimental Science and ENgineering (IJCESEN)

Vol. 11-No.3 (2025) pp. 5808-5819
http://www.ijcesen.com

ISSN: 2149-9144

Research Article

Multispectral Indices for Crop Water Stress Assessment and Precision Irrigation in Arid Agriculture: A Case Study from Béchar, Algeria

Benyamina Ahmed[1*], Grioui Hanane[2]

[1]Department of Computer Science, Faculty of Exact Sciences, Tahri Mohammed University, Bechar, Algeria
*** Corresponding Author Email:** benyamina.ahmed@univ-bechar.dz – **ORCID**: 0000-0002-6710-6462.

[2]Department of Computer Science, Faculty of Exact Sciences, Tahri Mohammed University, Bechar, Algeria
Email: grioui.hanane@univ-bechar.dz - **ORCID**:0009-0009-8021-0385

Article Info:

DOI: 10.22399/ijcesen.3414
Received : 10 May 2025
Accepted : 17 July 2025

Keywords

Precision irrigation
Remote sensing
Water stress
Multispectral imagery
Arid agriculture

Abstract:

Water scarcity combined with increasing food demand poses significant challenges to agricultural sustainability, particularly in arid regions such as Béchar province in Algeria, where irrigation accounts for approximately 70% of total water consumption. This study presents an innovative satellite-based precision irrigation system leveraging multispectral imagery from Landsat 8 and Sentinel-2 satellites to optimize water use efficiency while maintaining crop productivity. The proposed approach integrates multiple biophysical indices, including Land Surface Temperature (LST), Normalized Difference Vegetation Index (NDVI), Automated Water Extraction Index (AWEI), and Soil Moisture Index (SMI), to accurately assess crop water stress and irrigation requirements in near real-time. Validation was conducted over four agricultural seasons within the Ouakda zone, encompassing 17 crop types such as lettuce, beetroot, and turnip, over an area of 5.33 km². Results indicate a strong correlation between NDVI values and water stress levels: NDVI below 0.33 signals critical irrigation needs, whereas values above 0.66 correspond to optimal vegetation health. Land cover classification revealed a vegetation coverage of 36.3%, while spectral indices effectively tracked seasonal variations in crop vigor. Winter crops demonstrated enhanced growth under regulated irrigation regimes, whereas summer crops exhibited pronounced water stress. This system delivers actionable irrigation recommendations that could reduce water consumption by up to 30% without compromising yields. By combining remote sensing data with multispectral analysis, this research offers a scalable, adaptable framework for precision irrigation in arid environments, fostering sustainable water management and agricultural resilience. The methodology holds potential for global application in similar water-scarce agroecosystems.

1. Introduction

In the face of an accelerating global water crisis and an ever-expanding population demanding food security, agriculture stands at a critical crossroads. The stark reality is unmistakable: irrigation consumes approximately 70% of the world's freshwater resources, yet agricultural productivity must increase by 60% by 2050 to feed an estimated 9.7 billion people. This paradox is particularly acute in arid and semi-arid regions, where water scarcity severely constrains agricultural development while the need for food production intensifies. The Mediterranean basin, North Africa, and similar water-stressed regions exemplify this challenge, where traditional irrigation practices often result in substantial water waste while failing to optimize crop yields.

Algeria, like many countries in the Middle East and North Africa (MENA) region, faces mounting pressure to revolutionize its agricultural water management systems. With over 80% of its territory classified as arid or semi-arid, and precipitation patterns becoming increasingly erratic due to climate change, the country's agricultural sector must urgently transition toward precision irrigation strategies. The Béchar province, located in southwestern Algeria, epitomizes these challenges. Here, agricultural communities have traditionally relied on flood irrigation and intuitive farming practices that, while culturally significant,

often lead to over-irrigation in some areas and under-irrigation in others, resulting in both water waste and suboptimal crop performance.

The emergence of precision agriculture represents a paradigm shift from conventional farming toward data-driven, technology-enhanced agricultural practices. This transformation is powered by the convergence of several technological revolutions: the proliferation of satellite remote sensing capabilities, advances in geographic information systems (GIS), the Internet of Things (IoT), machine learning algorithms, and increasingly sophisticated sensor networks [5][6][8][10]. Among these technologies, satellite remote sensing has emerged as particularly promising for irrigation management [1][22], offering the unique ability to monitor vast agricultural areas with high temporal frequency and spatial resolution, providing insights that were previously impossible to obtain through ground-based methods alone.

Remote sensing technology for agricultural applications has evolved dramatically over the past two decades [18]. Early applications focused primarily on basic vegetation monitoring and land cover classification. However, recent advances in sensor technology, data processing capabilities, and analytical methods have enabled sophisticated applications including real-time crop health assessment, soil moisture estimation, irrigation scheduling optimization, and yield prediction [12][21][23]. The launch of high-resolution satellites such as Landsat 8 in 2013 and the Sentinel-2 constellation beginning in 2015 has democratized access to high-quality earth observation data, making precision agriculture applications feasible for researchers and farmers worldwide [20].

The theoretical foundation of satellite-based irrigation monitoring rests on the principle that different land surfaces and vegetation conditions exhibit distinct spectral signatures across various electromagnetic wavelengths. Healthy, well-irrigated vegetation typically shows high reflectance in the near-infrared spectrum while absorbing strongly in the visible red spectrum, forming the basis for vegetation indices such as the Normalized Difference Vegetation Index (NDVI) [14]. Similarly, land surface temperature measurements derived from thermal infrared bands can indicate water stress conditions, as water-stressed vegetation typically exhibits higher temperatures due to reduced evapotranspiration.

The integration of multiple spectral indices—including vegetation indices, water indices, and thermal measurements—provides a comprehensive picture of crop water status and irrigation needs. The development of spectral indices specifically designed for irrigation monitoring has been a significant advancement in this field. Beyond the widely-used NDVI, researchers have developed specialized indices such as the Normalized Difference Water Index (NDWI), the Soil Moisture Index (SMI), and the Temperature Vegetation Dryness Index (TVDI) [14][16].

However, despite these technological advances, significant gaps remain in the practical application of satellite-based irrigation monitoring, particularly in developing regions where the need is most acute [9][24]. Many existing studies have focused on large-scale agricultural systems in developed countries, with limited attention to smallholder farming systems or arid region agriculture. Furthermore, most research has concentrated on single-season analyses or specific crop types, lacking the comprehensive, multi-seasonal approach necessary to understand the complex interactions between climate, soil, crops, and irrigation practices in water-limited environments.

The integration of multiple satellite platforms presents both opportunities and challenges. While Landsat 8 provides excellent thermal infrared capabilities, Sentinel-2 offers superior spatial resolution and additional spectral bands in the red-edge region. The complementary use of these platforms can provide more robust and frequent observations than either system alone, but requires sophisticated data fusion techniques and careful consideration of temporal and spatial registration issues [16][17].

Ground validation remains a critical component of any satellite-based monitoring system. While remote sensing can provide broad spatial coverage and frequent temporal observations, the accuracy and reliability of satellite-derived information must be validated through field measurements and farmer observations. This validation process is particularly important in developing regions where local environmental conditions, farming practices, and crop varieties may differ significantly from those in regions where satellite-based methods were originally developed and tested.

The socio-economic context of precision agriculture adoption in developing regions adds another layer of complexity to this challenge [9]. While satellite data and analytical tools are becoming increasingly accessible, the successful implementation of precision irrigation systems requires not only technological infrastructure but also farmer education, extension services, and economic incentives.

Climate change impacts further underscore the urgency of developing robust irrigation monitoring systems. Increasing temperature, changing precipitation patterns, and more frequent extreme

weather events are already affecting agricultural productivity in many regions. Traditional irrigation scheduling methods based on historical climate data and empirical rules are becoming less reliable as climate conditions shift [14][15][24]. Satellite-based monitoring systems offer the potential for adaptive irrigation management that can respond to changing conditions in real-time.

2. Methodology

2.1 Study Area

The study was carried out in the Ouakda agricultural zone, located in Béchar province in southwestern Algeria (Figure 1). The precise site corresponds to the "Ouakda urban area, Section 114, Property Group No. 128, Béchar," a privately owned farm belonging to Mr. Kabbab Mohammed. This region is representative of arid agro-ecological zones, where agricultural productivity is severely challenged by water scarcity, high evapotranspiration rates, and pronounced climatic variability. Béchar was deliberately chosen as the study location due to its atypical seasonal dynamics—where the length and onset of seasons frequently deviate from conventional patterns—posing additional complexity to crop water management and irrigation scheduling.

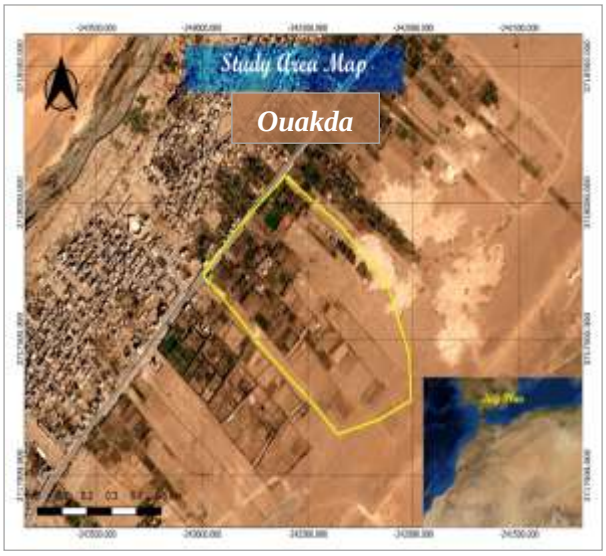

***Figure 1**. Study area map (Ouakda).*

The Ouakda farms, characterized by diverse crop types and varying irrigation practices, present an ideal setting for remote sensing-based irrigation monitoring. With an approximate coverage of 5.33 km², this agricultural zone exemplifies the broader challenges faced in arid environments and aligns with previous studies focused on sustainable irrigation in such regions [9][24].

2.2.1 Satellite Data

This study employed multi-temporal satellite imagery from two major platforms—**Landsat 8** and **Sentinel-2**—chosen for their complementary spectral and spatial capabilities.

Landsat 8 Dataset [21]:

- **Launch year**: 2013
- **Spectral bands**: 11
- **Key features**:
- Ensures continuity of the Landsat program since 1972
- Provides systematically archived global data (Global Survey Mission)
- Offers free, radiometrically and geometrically calibrated data through the USGS Earth Resources Observation and Science (EROS) Center
- Delivers standard products with radiometric uncertainty below 5%
- Enables near-immediate product download

Sentinel-2 Dataset [20]:

- **Launch year**: 2015 (Sentinel-2A)
- **Swath width**: 290 km
- **Spectral bands**: 13
- **Spatial resolution**:
    - Four visible and near-infrared (NIR) bands at 10 m
    - Six red-edge and shortwave infrared (SWIR) bands at 20 m
    - Three atmospheric bands for correction at 60 m
- Offers high revisit frequency and superior red-edge sensitivity, making it highly suitable for vegetation and soil moisture monitoring.

2.2.2 Ground Truth Data

A comprehensive ground-truthing campaign was conducted throughout the Ouakda agricultural zone to support the remote sensing analysis. Field surveys enabled the identification and georeferencing of **seventeen distinct land cover classes** (Figure 2), serving as essential reference data for the supervised classification process. These in-situ observations were subsequently used to train the classification algorithm and to assess its performance through **confusion matrix analysis**, providing a robust basis for evaluating classification accuracy.

- **Crops**: lettuce, beet, turnip, carrots, garlic, tomato, pepper, eggplant, mint, barley, beans [11]

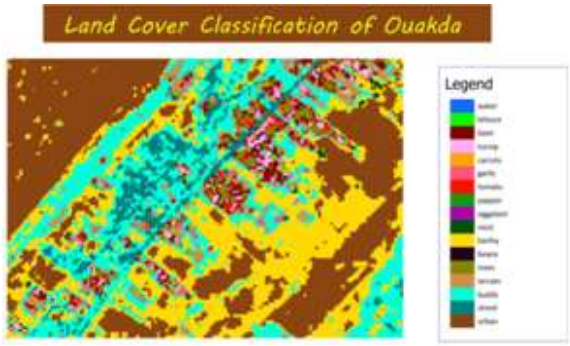

Figure 2: *Land cover classification of Ouakda.*

- **Other features**: water, trees, terrain, buildings, street, urban areas

Precise positioning data (X1, Y1, X2, Y2 coordinates) and frequency information were collected for each class to support supervised classification and validation processes.

2.3 Image Pre-Processing [12]

The satellite imagery underwent standard pre-processing procedures including:

1. **Atmospheric Correction**: Applied to both Landsat 8 and Sentinel-2 data to remove atmospheric effects
2. **Geometric Correction**: Ensuring proper spatial alignment between different temporal acquisitions
3. **Radiometric Calibration**: Converting digital numbers to Top of Atmosphere (TOA) reflectance values
4. **Cloud Masking:** Identifying and removing cloud-contaminated pixels
5. **Temporal Registration**: Aligning multi-temporal datasets for consistent analysis

2.4 Image Processing

To quantitatively assess vegetation health, water stress, and soil moisture dynamics, spectral indices derived from multispectral satellite imagery were calculated (table 1). The formulations of these indices differ between **Landsat 8** and **Sentinel-2** due to variations in spectral band configurations, particularly in terms of central wavelengths and spatial resolutions [21][20]. **Table 1** summarizes the mathematical expressions of key indices—including **NDVI**, **NDWI**, **EVI**, **SAVI** [12], and **AWEI**—adapted for both sensors to ensure cross-platform consistency in irrigation monitoring. These indices were selected based on their demonstrated effectiveness in arid-land agriculture, where they have been widely used for detecting vegetation vigor, monitoring drought stress, and extracting surface water features [14][16][24]. The use of open-access satellite data further reinforces the operational feasibility of these indices in resource-limited regions.

Table 1: *Spectral indices formula*

Index
NDVI = $\frac{NIR - RED}{NIR+RED}$
NDBI = $\frac{SWIR - NIR}{SWIR+NIR}$
NDWI = $\frac{NIR - SWIR}{NIR+SWIR}$
EVI=2.5*($\frac{NIR - R}{NIR + (6 * R) - (7.5 * B) + 1}$**)**
EVI2=2.5*($\frac{NIR - R}{NIR + (6 * R) - (2.4 * R) + 1}$**)**
SAVI = $\frac{(NIR - \mathrm{RED})\,(1-L)}{(NIR+RED+L)}$
AWEI = 4 * (Green – SWIR2) – (0.25 * NIR + 2.75 * SWIR1)

2.4.1 Spectral Indices Calculation

A range of spectral indices were derived from both **Landsat 8** (Table 2) and **Sentinel-2** (Table 3) imagery to support the analysis. These indices were selected for their relevance in assessing vegetation vigor, soil moisture, and crop water stress under arid conditions.

2.4.1.1 Vegetation Indices:

- **NDVI (Normalized Difference Vegetation Index):**
- **EVI (Enhanced Vegetation Index):**
- **SAVI (Soil Adjusted Vegetation Index):** Where L is the soil brightness correction factor

2.4.1.2 Water and Moisture Indices:

- **NDWI (**Normalized Difference Water Index**)**
- **AWEI (**Automated Water Extraction Index**)**
- **SMI (Soil Moisture Index)**: Calculated to assess soil water content

2.4.1.3 Thermal Indices:

- **LST (**Land Surface Temperature**):** Derived from thermal infrared bands
- **TVDI (**Temperature Vegetation Dryness Index**):** Calculated using NDVI and LST for identifying water stress conditions

Table 2: *Spectral indices formula using landsat*

Index
NDVI = $\frac{band5 - band4}{band5 + band4}$
NDBI = $\frac{band6 - band5}{band6 + band5}$
NDWI = $\frac{band5 - band6}{band5 + band6}$
EVI=2.5*($\frac{band5 - band4}{b5 + (6 * b4) - (7.5 * b2) + 1}$)
EVI2=2.5* ($\frac{band5 - band4}{b5 + (6 * b4) - (2.4 * b4) + 1}$)
SAVI = $\frac{(band5 - band4)\,(1-L)}{(band5 + band4 + L)}$
AWEI = 4 * (band3 – band12) – (0.25 * band8+ 2.75 * band11)

Table 3: *Spectral indices formula using sentinel 2*

Index
NDVI = $\frac{band8 - band4}{band8 + band4}$
DBI = $\frac{band11 - band8}{band11 + band8}$
NDWI = $\frac{band8 - band11}{band8 + band11}$
EVI=2.5*($\frac{band8 - band4}{b8 + (6 * b4) - (7.5 * b2) + 1}$)
EVI2=2.5* ($\frac{band8 - band4}{b8 + (6 * b4) - (2.4 * b4) + 1}$)
SAVI = $\frac{(band8 - band4)\,(1-L)}{(band8 + band4 + L)}$
AWEI = 4 * (band3 – band7) – (0.25 * band5 + 2.75 * band6)

2.4.2 Multi-temporal Analysis

Four seasonal datasets were analyzed [3]:
- Winter: March 2, 2025
- Autumn: December 1, 2024
- Spring: May 8, 2024
- Summer: August 11, 2024

This temporal approach allowed for comprehensive assessment of seasonal variations in crop water requirements and irrigation patterns.

2.5 Images Classification

2.5.1 Supervised Classification Approach [17]

A supervised classification methodology was implemented using:
- **Training Data**: Ground truth information collected from field surveys
- **Classification Algorithm**: Applied to distinguish between different land cover types
- **Spectral Signature Analysis**: Utilizing the distinct electromagnetic signatures of different surfaces

2.5.2 Land Cover Classes

The classification scheme included 17 distinct classes with their respective characteristics [11]:
- **Agricultural classes**: Various crop types with specific spectral and temporal signatures
- **Non-agricultural classes**: Urban areas, buildings, streets, water bodies, and natural terrain

2.5.3 Irrigation Status Classification

The primary objective focused on distinguishing between [1][3][21]:
- **Irrigated areas**: Characterized by higher vegetation indices, lower land surface temperatures, and higher soil moisture
- **Non-irrigated areas:** Showing water stress indicators through spectral analysis

2.5.4 Accuracy Assessment Framework

Classification accuracy was evaluated through [4]:
- **Confusion Matrix Analysis**: Comparing classified results with ground truth data
- **Statistical Validation:** Using field measurements for validation
- **Cross-validation Techniques**: Ensuring robustness of classification results

The methodology integrated synchronous measurements of LST, NDVI, AWEI, and SMI based on satellite imagery from Landsat 8 and Sentinel-2, providing a comprehensive framework for distinguishing between irrigated and non-irrigated agricultural areas and supporting precision irrigation decision-making.

3. Results and Discussion

3.1 Assessment of Classification Accuracy

The study implemented a supervised classification of satellite images (Landsat 8 and Sentinel 2) to map land cover in the Ouakda agricultural area, Béchar. Land cover data was collected directly from the field, enabling detailed identification of vegetation types and land use (17 classes, including

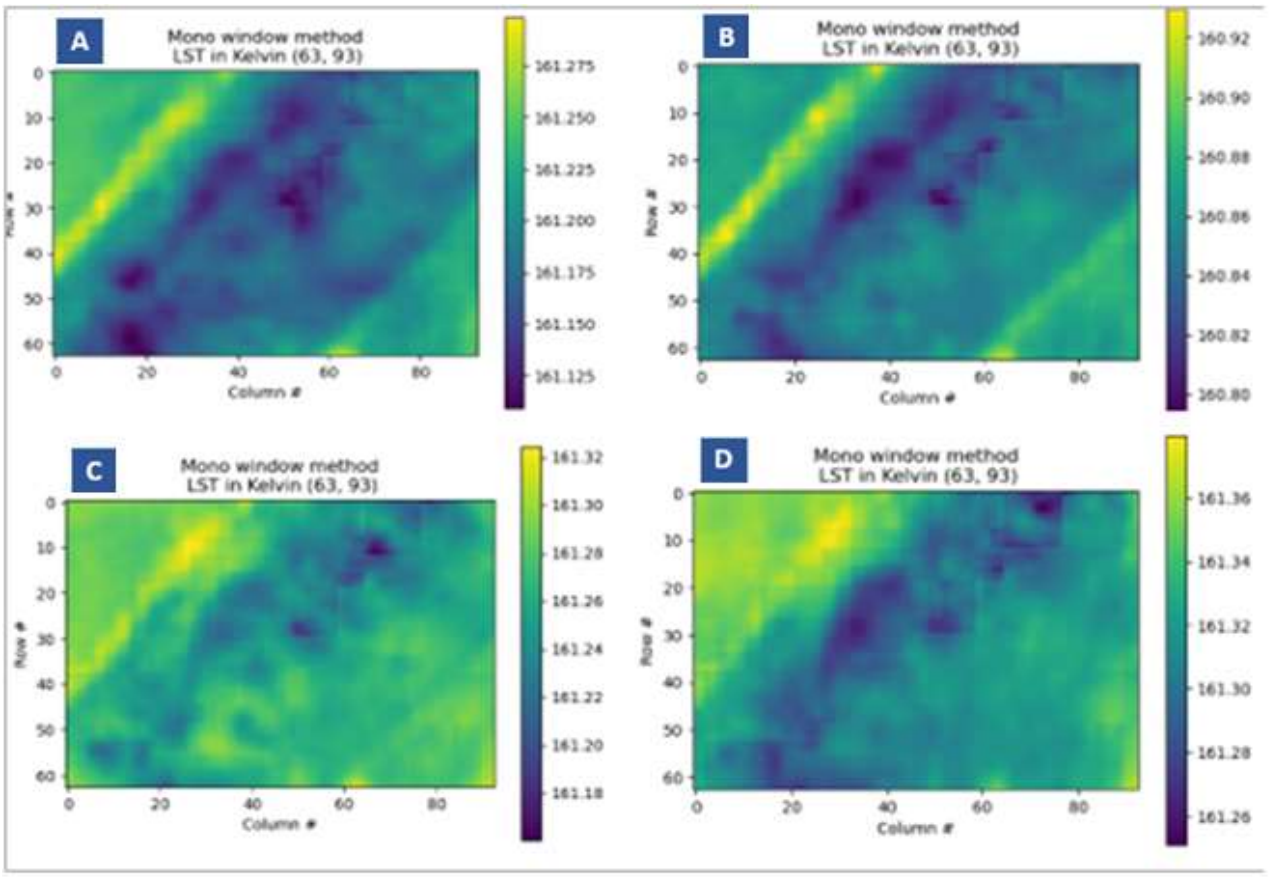

Figure 3: *LST of (A): winter, (B) autumn, (C) spring, (D) summer.*

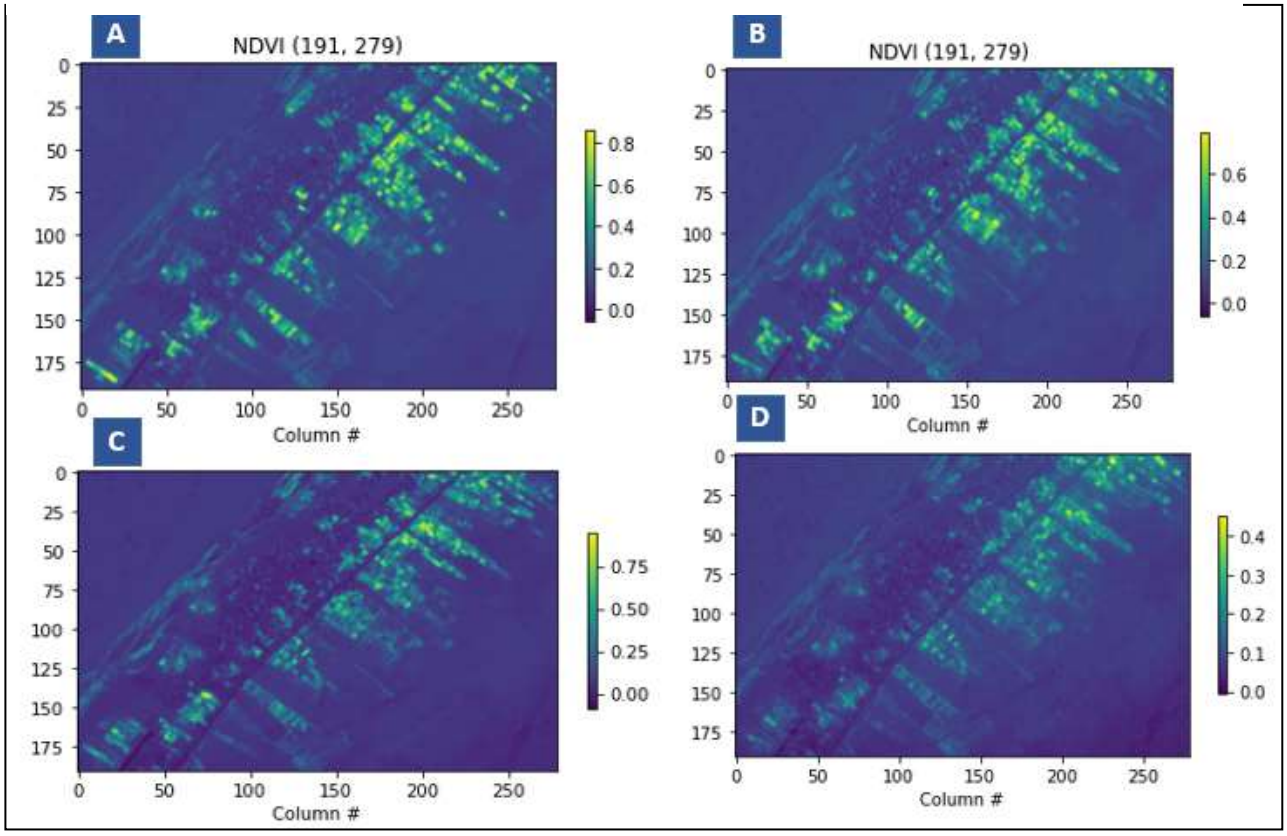

Figure 4: *NDVI of (A): winter, (B) autumn, (C) spring, (D) summer*

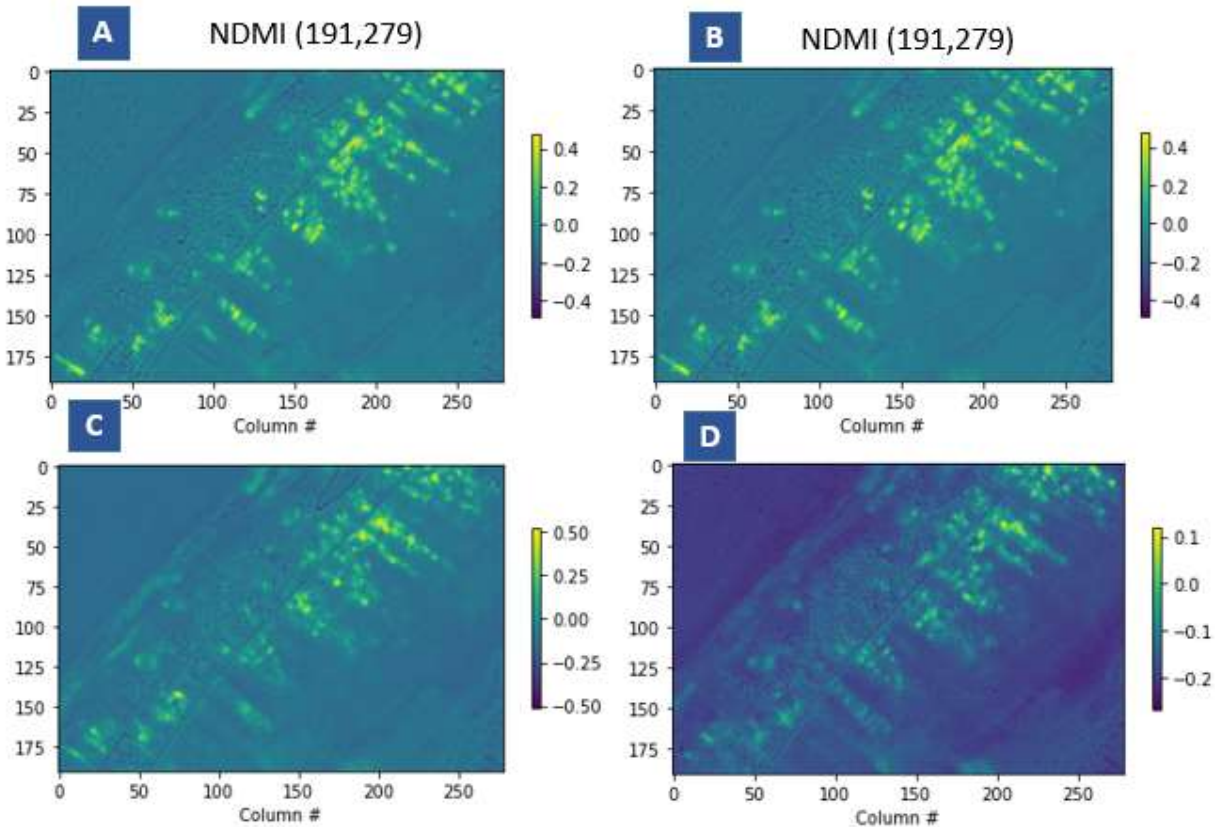

Figure 5: *NDMI of (A): winter, (B) autumn, (C) spring, (D) summer.*

water, lettuce, beet, turnip, carrots, garlic, tomato, pepper, eggplant, mint, barley, beans, trees, bare soil, buildings, street, and urban). The classification results are presented in tables and histograms, showing the proportion of each class, the number of pixels, and the corresponding area.

The classification revealed that vegetation cover accounts for 36.3% of land use, including several vegetable crops (lettuce, beet, eggplants, turnip, etc.) [11]. A detailed breakdown of all land cover categories is provided in **Table 2: Classification classes data**. The accuracy of the classification was validated by comparing the results with ground reference data, and the outputs are visualized through maps and figures as illustrated in Figure 2 the Ouakda region is mostly dominated by agricultural land.

3.2 Detection of Spatial-Temporal Changes

Spatial-temporal changes were detected using spectral indices calculated for different seasons (winter, autumn, spring, summer): LST (Land Surface Temperature), NDVI (Normalized Difference Vegetation Index), NDMI (Normalized Difference Moisture Index), SMI (Soil Moisture Index), and TVDI (Temperature Vegetation Dryness Index). These indices were extracted and analyzed for each season, allowing the monitoring of vegetation status and soil moisture dynamics throughout the year.

The **seasonal variation of surface temperature** is clearly illustrated in **Figure 3**, which shows the LST distribution across winter, autumn, spring, and summer. Similarly, **Figure 4** presents the spatial distribution of NDVI, highlighting seasonal fluctuations in vegetation vigor, while **Figure 5** depicts the NDMI maps, reflecting changes in vegetation moisture content across seasons.

Key findings include:

- NDVI values range from -1 to 1, indicating vegetation health (from dead to very healthy).
- SMI distinguishes dry soils (0 to 0.5) from wet soils (0.5 to 1).
- Seasonal maps (**Figures 3–5**) illustrate variations in surface temperature, moisture, and vegetation vigor, helping to identify irrigated and non-irrigated areas and to detect changes due to agricultural practices or climatic conditions.

By combining classification results (Table 2) and spectral indices, the study enabled detailed mapping and monitoring of irrigation zones, supporting decision-making for precision agriculture and water management. The integration of thermal imagery and spectral indices into an intelligent monitoring system provided significant improvements in mapping, monitoring, and analyzing irrigated areas,

especially in optimizing water use and maintaining crop health.

This project presents an intelligent irrigation monitoring system that guides and helps the farmer to take the decision from thermal image by mixing classification land cover result with spectral indices results, these indices made promising improvement through mapping, monitoring and analysing. From land cover classification mapping and spectral remote sensing indices, we monitor irrigation zones levels, land cover result determine vegetation cover correctly 36.3% of land use, the vegetation consist of several vegetables including: lettuce, beet, eggplants, turnip.

Table 2: *Classification classes data.*

N°	Class	PixelSum	Percentage %	Area [m^2]
1	Lettuce	249	0.47	24900
2	Beet	1093	2.05	109300
3	Turnip	616	1.16	61600
4	Carrots	229	0.43	22900
5	Garlic	1223	2.30	122300
6	Tomato	455	0.85	45500
7	Papper	149	0.28	14900
8	Eggplant	103	0.19	10300
9	Mint	327	0.61	32700
10	Trees	855	1.60	85500
11	Terrain	2205	4.14	220500
12	Builds	11302	21.21	1130200
13	Street	2756	5.17	275600
14	Urban	17831	33.46	1783100
15	Barley	13673	25.66	1367300
16	Beans	223	0.42	22300

3.3 Crop-specific Seasonal Analysis

The NDVI ranges from -1 to 1: values below 0 indicate no vegetation, values between 0 and 0.33 correspond to unhealthy vegetation, 0.33 to 0.66 indicates moderate vegetation health, and values above 0.66 reflect very healthy vegetation.

SMI range is from 0 to 0.5 means dry soil and from 0.5 to 1 wet soil.

Lettuce, for example, is a typical winter vegetable that thrives in cool weather and abundant sunlight. It grows best in nitrogen-rich soil and requires consistently moist conditions to stay healthy, we used NDVI, LST, and SMI values collected across four seasons—winter (03/02/2022), autumn (01/12/2021), spring (08/05/2021), and summer (11/08/2021)—to assess the seasonal behavior of lettuce, we analyzed the lettuce-specific indices, and the seasonal results are summarized as follows:

Lettuce	NDVI	LST	SMI
Winter	0.6	-109.16	0.7
Autumn	0.5	-111.40	0.5
Spring	0.7	-110.80	0.2
Summer	0.3	-110.96	0.2

Lettuce indices results (NDVI vs SMI and LST) histograms:

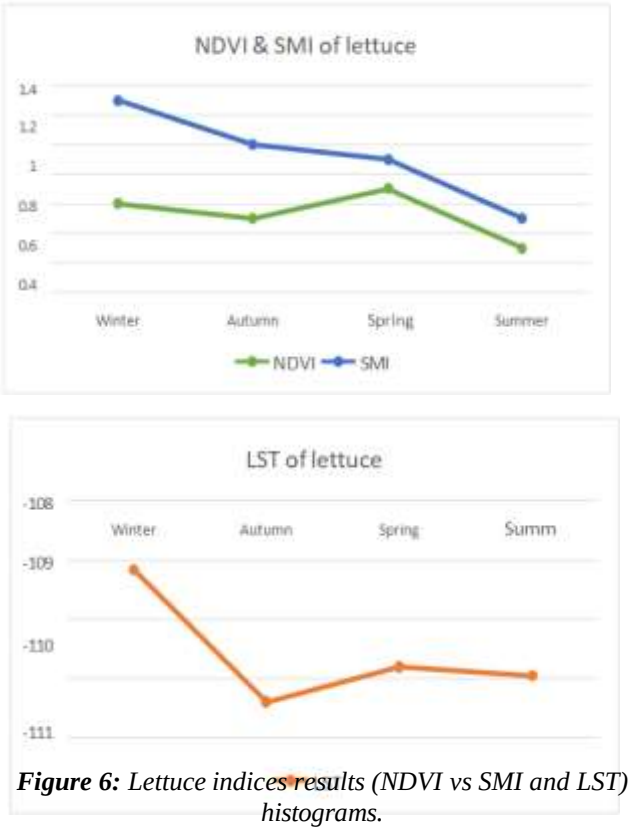

Figure 6: *Lettuce indices results (NDVI vs SMI and LST) histograms.*

In winter, lettuce exhibited healthy growth under conditions of high humidity and low temperature, indicating that it was regularly irrigated. However, excessive soil moisture may have increased the risk of disease, potentially affecting up to 80% of the crop.

In autumn, lettuce remained healthy despite high temperatures and moderate humidity, indicating moderate irrigation. However, signs of early drought stress suggest that irrigation levels should be increased to maintain optimal crop conditions.

In spring, lettuce showed very healthy growth under dry conditions and moderate temperatures, suggesting that it was not irrigated but still

maintained good physiological performance.

In summer, lettuce appeared unhealthy under dry conditions and moderate temperatures. The lack of irrigation likely led to severe damage—up to 98%—due to plant disease triggered by irregular irrigation practices that caused fluctuations in soil moisture.

Lettuce typically grows during the spring and summer seasons. The results indicate that it was regularly irrigated in spring, whereas the damage observed in summer confirms that irregular irrigation negatively affected its growth, quality, and overall productivity. These seasonal dynamics are clearly visualized in **Figure 6**, which presents histograms of NDVI, SMI, and LST values for lettuce across the four seasons, highlighting the correlation between vegetation health, soil moisture, and surface temperature.

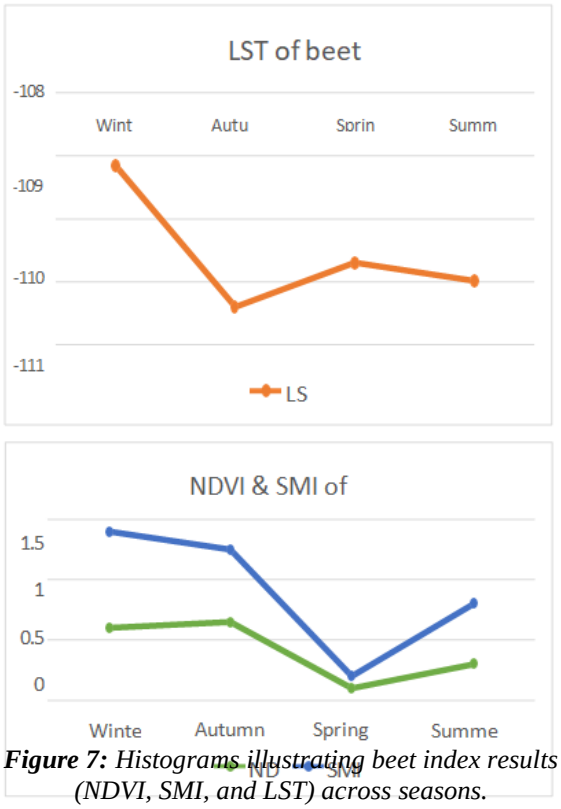

Figure 7: *Histograms illustrating beet index results (NDVI, SMI, and LST) across seasons.*

Beet and lettuce share similar environmental requirements and growth characteristics.

The seasonal NDVI values for beet are summarized as follows:

Beet	NDVI	LST	SMI
Winter	0.6	-109.16	0.8
Autumn	0.65	-111.40	0.6
Spring	0.1	-110.70	0.1
Summer	0.3	-110.98	0.5

It is known that beet grows well under similar conditions in winter, autumn, and spring, but not in summer. Under moderate temperatures and drought conditions, beet appeared unhealthy. The absence of irrigation likely resulted in up to 98% crop damage due to diseases triggered by irregular irrigation practices.

Beet is a vegetable that requires regular irrigation to maintain healthy growth. Beet typically grows during the spring and summer seasons. The results show that it was regularly irrigated in autumn; however, the significant damage observed in summer confirms that irregular irrigation negatively affected its growth, quality, and productivity.

These seasonal variations in vegetation vigor, soil moisture, and surface temperature for beet are illustrated in **Figure 7**, which presents histograms of NDVI, SMI, and LST values across the four seasons.

Turnip is a winter-season crop that relies on regular irrigation. Its successful growth depends on maintaining adequate soil moisture and overall soil health. The NDVI results for turnip across different seasons are summarized as follows, and are illustrated in **Figure 8**, which presents histograms of NDVI, SMI, and LST values for turnip throughout the year.

Turnip	NDVI	LST	SMI
Winter	0.8	-109.20	0.9
Autumn	0.7	-111.45	0.7
Spring	0.1	-110.01	0.1
Summer	0.1	-110.98	0.6

Histograms showing turnip index results (NDVI, SMI, and LST) across seasons:

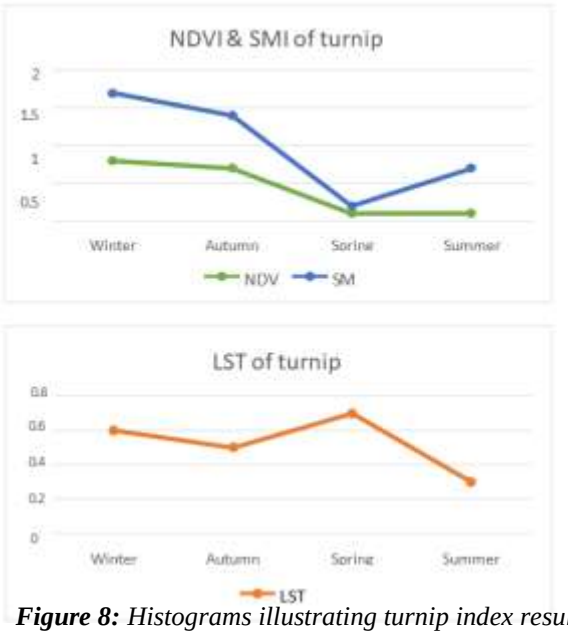

Figure 8: *Histograms illustrating turnip index results (NDVI, SMI, and LST) across seasons.*

In winter, turnip exhibited very healthy growth

under high humidity and low temperatures, indicating that it was well irrigated and consistently exposed to regular watering.

In autumn, turnip remained healthy despite high temperatures and elevated humidity, suggesting that it was regularly irrigated and able to meet its increased water demands.

In spring, turnip appeared unhealthy under dry conditions and high temperatures. The lack of regular irrigation likely led to approximately 98% crop damage due to plant diseases triggered by reduced soil moisture from inconsistent watering.

In summer, turnip showed poor health despite the presence of humidity and moderate temperatures. Although irrigation was applied, the crop did not respond effectively, resulting in approximately 98% damage. This was likely due to plant diseases caused by irregular irrigation and soil degradation.

Turnip is a winter-season crop that relies on regular irrigation and requires careful management of soil moisture and overall soil health. Turnip is a fast-growing plant that requires a specific irrigation interval of approximately every 10 days. It thrives under moderate temperatures and high soil moisture conditions. During the vegetative growth phase, turnip plants perform best under moderately warm temperatures. However, during the root swelling stage, they require cooler conditions. This explains why turnip achieves its highest productivity and quality in winter. In contrast, productivity is lower in spring and autumn, primarily due to irregular irrigation practices that negatively impact soil moisture levels.

4. Conclusion

This study demonstrates the effectiveness of integrating satellite remote sensing data with advanced spectral indices for intelligent irrigation monitoring in arid agricultural environments. By combining supervised land cover classification using multi-spectral imagery (Landsat 8 and Sentinel-2) with the calculation of key indices such as NDVI, LST, SMI, NDMI, and TVDI across different seasons, it was possible to accurately distinguish irrigated from non-irrigated areas and monitor crop health and soil moisture dynamics. The developed system enabled precise mapping of land cover—revealing vegetation coverage of 36.3%—and provided actionable insights into the spatial and temporal variability of crop conditions. Crop-specific seasonal analysis further demonstrated how spectral indices can detect vegetation stress, soil moisture fluctuations, and the effects of irregular irrigation, particularly for sensitive crops like lettuce, beet, and turnip. Analysis of LST, NDVI, and SMI confirmed a strong positive correlation: as soil moisture increased, plant health improved, ultimately enhancing crop quality and productivity. These findings underscore the critical role of regular irrigation in maximizing agricultural performance. Overall, the integration of remote sensing technologies with intelligent data analysis offers a robust, scalable, and non-destructive solution for optimizing irrigation practices. This approach enhances water use efficiency, supports sustainable resource management, and reinforces the strategic value of remote sensing in the advancement of precision agriculture, especially in water-scarce regions.

Author Declarations

- **Ethical Approval**: This research did not involve human participants or animal subjects, and thus no ethical approval was required.
- **Conflict of Interest**: The authors declare that they have no known competing financial interests or personal relationships that could have appeared to influence the work reported in this paper.
- **Acknowledgments**: The authors have no individuals or organizations to acknowledge for contributions to this work.
- **Author Contributions**: All authors contributed equally to the conception, methodology, analysis, and writing of this manuscript.
- **Funding**: This study did not receive any specific grant from funding agencies in the public, commercial, or not-for-profit sectors.
- **Data Availability**: The satellite datasets used in this study (Landsat 8 and Sentinel-2) are publicly available from the USGS Earth Explorer and the Copernicus Open Access Hub, respectively. Ground-truth data collected during the field surveys are not publicly available due to privacy and geolocation sensitivity, but can be made available by the corresponding author upon reasonable request.

References

[1] Li, Y., & Liu, X. (2024). Surface water extraction from remote sensing images of arid regions in Africa using a deep learning approach combining multiscale information. *Proceedings of SPIE, 12565*, 125650F. https://doi.org/10.1117/12.3045960.

[2] Call, A., Akiba, S., & Pringle, E. G. (2024). Remote sensing reveals the importance of seminatural habitat and irrigation on aphid biocontrol in arid agroecosystems. *Ecological*

Solutions and Evidence, *5*(2), e12377. https://doi.org/10.1002/2688-8319.12377.

[3] Zhang, M., Zhang, H., Deng, W., & Yuan, Q. (2024). Assessment of habitat quality in arid regions incorporating remote sensing data and field experiments. *Remote Sensing*, *16*(19), 3648. https://doi.org/10.3390/rs16193648.

[4] Md-Tahir, H., Mahmood, H. S., Husain, M., Khalil, A. A., Shoaib, M., Ali, M., Ali, M. M., Tasawar, M., Khan, Y., Awan, U. K., & Cheema, M. J. M. (2024). Localized crop classification by NDVI time series analysis of remote sensing satellite data: Applications for mechanization strategy and integrated resource management. *AgriEngineering*, *6*(3), 2429–2444. https://doi.org/10.3390/agriengineering6030142.

[5] Parra-López, C., Abdallah, S. B., Garcia-Garcia, G., Hassoun, A., Trollman, H., Jagtap, S., & others. (2025). *Digital technologies for water use and management in agriculture: Recent applications and future outlook* [Manuscript submitted for publication]. University of Leicester. https://hdl.handle.net/2381/28333481.v1.

[6] Ambaru, B., Manvitha, R., & Madas, R. (2025). Synergistic integration of remote sensing and soil metagenomics data: advancing precision agriculture through interdisciplinary approaches. *Frontiers in Sustainable Food Systems*, *8*. https://doi.org/10.3389/fsufs.2024.1499973.

[7] Guo, L., Chao, X., Wu, H., Shi, M., & Fan, Y. (2024). The Decisive Influence of the Improved Remote Sensing Ecological Index on the Terrestrial Ecosystem in Typical Arid Areas of China. *Land*, *13*(12), 2162. https://doi.org/10.3390/land13122162.

[8] Handoko, E. Y., Fahriza, A., & Muryono, M. (2024). *Integrating Remote Sensing and GIS for Precision Agriculture: Leveraging Google Earth Engine for Enhanced Agricultural Management*. *1418*, 012054. https://doi.org/10.1088/1755-1315/1418/1/012054.

[9] Ouédraogo, S., Kabre, S., Somda, W., Kébré, M. B., & Zougmoré, F. (2024). *Sustainable Irrigation and Fertilization Strategies for Maize in Arid Regions: Insights from Numerical Modeling and Simulation*. 1–9. https://doi.org/10.1109/mne3sd63831.2024.10812157.

[10] Frontiers in Plant Science. (2025). Sustainable and Intelligent Phytoprotection. *Frontiers in Plant Science, 16*, Article 1587869. https://doi.org/10.3389/fpls.2025.1587869.

[11] Meshram, P. G., Shaniware, Y., Bhondave, G. P., Zol, D. M., & Pandey, P. (2024). Precision Agriculture: UAV-Based Soil Mapping and Remote Sensing Applications. *Asian Research Journal of Agriculture*. https://doi.org/10.9734/arja/2024/v17i4598

[12] **Zhou, M., Wang, X., Liu, W., & Li, J. (2023).** *Soil salinity mapping using Sentinel-2 data and machine learning in an arid irrigation district of China*. *Remote Sensing*, *15*(1), 187. https://doi.org/10.3390/rs15010187

[13] **Jancevičius, J. (2025).** *Enhancing land use classification with hybrid machine learning and satellite imagery. New Trends in Computer Sciences*, *3*(1), 1–17. https://doi.org/10.3846/ntcs.2025.23701

[14] Karnieli, A., Agam, N., Pinker, R., Anderson, M., Imhoff, M., Gutman, G., Panov, N., & Goldberg, A. (2010). *Use of NDVI and land surface temperature for drought assessment: Merits and limitations. Journal of Climate*, *23*(3), 618–633. https://doi.org/10.1175/2009JCLI2900.1

[15] Folhes, M., Rennó, C. D., & Soares, J. V. (2009). *Remote sensing for irrigation water management in the semi-arid Northeast of Brazil. Agricultural Water Management*, *96*(10), 1398–1408. https://doi.org/10.1016/j.agwat.2009.04.021

[16] Saadi, S., Simonneaux, V., Boulet, G., Raimbault, B., Mougenot, B., Fanise, P., Ayari, H., & Lili-Chabaane, Z. (2015). Monitoring Irrigation Consumption Using High Resolution NDVI Image Time Series: Calibration and Validation in the Kairouan Plain (Tunisia). *Remote Sensing*, *7*(10), 13005-13028. https://doi.org/10.3390/rs71013005.

[17] Niazmardi, S., Homayouni, S., Safari, A., McNairn, H., Shang, J., & Beckett, K. (2018). Histogram-based spatio-temporal feature classification of vegetation indices time-series for crop mapping. *International Journal of Applied Earth Observation and Geoinformation*, *72*, 34–41. https://doi.org/10.1016/j.jag.2018.05.014

[18] Albertini, C., Gioia, A., Iacobellis, V., Petropoulos, G. P., & Manfreda, S. (2024). Assessing multi-source random forest classification and robustness of predictor variables in flooded areas mapping. *Remote Sensing Applications: Society and Environment*, *35*, Article 101239. https://doi.org/10.1016/j.rsase.2024.101239

[19] Belayhun, M., Chere, Z., Abay, N. G., Nicola, Y., & Asmamaw, A. (2024). Spatiotemporal pattern of water hyacinth (*Pontederia crassipes*) distribution in Lake Tana, Ethiopia, using a random forest machine learning model. *Frontiers in Environmental Science*, *12*, Article 1476014. https://doi.org/10.3389/fenvs.2024.1476014

[20] Kamenova, I., Chanev, M., Dimitrov, P., Filchev, L., Bonchev, B., Zhu, L., & Dong, Q. (2024). Crop type mapping and winter wheat yield prediction utilizing Sentinel-2: A case study from Upper Thracian Lowland, Bulgaria. *Remote Sensing*, *16*(7), Article 1144. https://doi.org/10.3390/rs16071144

[21] Farhadi, H., Ebadi, H., Kiani, A., & Asgary, A. (2024). Near real-time flood monitoring using multi-sensor optical imagery and machine learning by GEE: An automatic feature-based multi-class classification approach. *Remote Sensing*, *16*(23), Article 4454. https://doi.org/10.3390/rs16234454.

[22] Purnamasari, D., Teuling, A. J., & Weerts, A. H. (2025). Identifying irrigated areas using land surface temperature and hydrological modelling: Application to the Rhine basin. *Hydrology and Earth System Sciences*, *29*, 1483–1503. https://doi.org/10.5194/hess-29-1483-2025.

[23] Yu, L., Xie, H., Xu, Y., Li, Q., Jiang, Y., Tao, H., & Aihemaiti, M. (2024). Identification and monitoring of irrigated areas in arid areas based on Sentinel-2 time-series data and a machine learning algorithm. *Agriculture, 14*(10), 1–23. https://doi.org/10.3390/agriculture14102023

[24] Cao, C., Zhu, X., Liu, K., Liang, Y., & Ma, X. (2025). Satellite-Observed Arid Vegetation Greening and Terrestrial Water Storage Decline in the Hexi Corridor, Northwest China. *Remote Sensing*, *17*(8), 1361. https://doi.org/10.3390/rs17081361.